ELSEVIER

Neurobiology of Aging 33 (2012) 1122.e23–1122.e39

NEUROBIOLOGY OF AGING

www.elsevier.com/locate/neuaging

Impaired TrkB receptor signaling contributes to memory impairment in APP/PS1 mice

Susanna Kemppainen[a], Tomi Rantamäki[b], André Jerónimo-Santos[c], Gregoire Lavasseur[d,e], Henri Autio[b], Nina Karpova[b], Elisa Kärkkäinen[a], Saara Stavén[a], Hugo Vicente Miranda[f], Tiago F. Outeiro[f,g,h], Maria J. Diógenes[c], Serge Laroche[d,e], Sabrina Davis[d,e], Ana M. Sebastião[c], Eero Castrén[b], Heikki Tanila[a,b,i,*]

[a] *A. I. Virtanen Institute, University of Eastern Finland, Kuopio, Finland*
[b] *Neuroscience Center, University of Helsinki, Helsinki, Finland*
[c] *Institute of Pharmacology and Neurosciences, Faculty of Medicine and Unit of Neurosciences, Institute of Molecular Medicine, University of Lisbon, Lisbon, Portugal*
[d] *CNRS, UMR 8195, Orsay, France*
[e] *Univ Paris-Sud, Centre de Neurosciences Paris-Sud, UMR 8195, Orsay, France*
[f] *Cell and Molecular Neuroscience Unit, Instituto de Medicina Molecular, Lisboa, Portugal*
[g] *Instituto de Fisiologia, Faculdade de Medicina da Universidade de Lisboa, Lisboa, Portugal*
[h] *Department of NeuroDegeneration and Restaurative Research, University Medizin Gottingen, Gottingen, Germany*
[i] *Department of Neurology, Kuopio University Hospital, Kuopio, Finland*

Received 19 July 2011; received in revised form 25 October 2011; accepted 4 November 2011

Abstract

Brain-derived neurotrophic factor (BDNF) plays an important role in neuronal plasticity, learning, and memory. Levels of BDNF and its main receptor TrkB (TrkB.TK) have been reported to be decreased while the levels of the truncated TrkB (TrkB.T1) are increased in Alzheimer's disease. We show here that incubation with amyloid-β increased TrkB.T1 receptor levels and decreased TrkB.TK levels in primary neurons. In vivo, APPswe/PS1dE9 transgenic mice (APdE9) showed an age-dependent relative increase in cortical but not hippocampal TrkB.T1 receptor levels compared with TrkB.TK. To investigate the role of TrkB isoforms in Alzheimer's disease, we crossed AP mice with mice overexpressing the truncated TrkB.T1 receptor (T1) or the full-length TrkB.TK isoform. Overexpression of TrkB.T1 in APdE9 mice exacerbated their spatial memory impairment while the overexpression of TrkB.TK alleviated it. These data suggest that amyloid-β changes the ratio between TrkB isoforms in favor of the dominant-negative TrkB.T1 isoform both in vitro and in vivo and supports the role of BDNF signaling through TrkB in the pathophysiology and cognitive deficits of Alzheimer's disease.

Keywords: BDNF; Tyrosine kinase receptor; Amyloid; Memory; Hyperactivity

1. Introduction

Neuropathologically, Alzheimer's disease (AD) is characterized by amyloid plaques and neurofibrillary tangles, but the most likely proximal cause for the most characteristic symptom of the early stage of the disease, impaired memory for recent events, is loss of synapses (Selkoe, 2002). The molecular mechanisms whereby accumulation of amyloid-β into the brain leads to synaptic loss are still incompletely known.

Neurotrophins, in particular brain-derived neurotrophic factor (BDNF) regulate neuronal survival, differentiation, and plasticity by activating the receptor tyrosine kinase TrkB (Huang and Reichardt, 2001). Reduced BDNF signaling

* Corresponding author at: A. I. Virtanen Institute, University of Eastern Finland, P.O. Box 1627, Neulaniementie 2, 70211 Kuopio, Finland. Tel.: +358-40-3552084; fax: +358-17-163030.
E-mail address: Heikki.Tanila@uef.fi (H. Tanila).

0197-4580/$ – see front matter © 2012 Elsevier Inc. All rights reserved.
doi:10.1016/j.neurobiolaging.2011.11.006

through TrkB leads to impaired spatial memory (Minichiello, 2009; Minichiello et al., 1999; Saarelainen et al., 2000b), while overexpression of TrkB enhances memory (Koponen et al., 2004). These observations have led to the suggestion that TrkB signaling might be involved in the pathophysiology of AD (Arancio and Chao, 2007; Castrén and Tanila, 2006; Schindowski et al., 2008; Zuccato and Cattaneo, 2009). BDNF messenger RNA (mRNA) and protein levels as well as protein levels for the full-length TrkB isoform have been found to be reduced in postmortem brain samples of AD patients (Connor and Dragunow, 1998; Connor et al., 1997; Ferrer et al., 1999; Phillips et al., 1991). In contrast, the truncated, dominant-negative isoform of TrkB (TrkB.T1) (Eide et al., 1996; Haapasalo et al., 2001) has been found to be increased (Connor et al., 1996; Ferrer et al., 1999). Importantly, BDNF levels are already reduced at the preclinical stages of the disease (Peng et al., 2005). Taken together, these findings implicate that BDNF signaling is impaired in AD patients. In contrast, studies in amyloid precursor protein (APP) transgenic mice modeling AD have yielded mixed results regarding brain BDNF levels (either mRNA or protein) with 2 lines displaying decreased levels (Peng et al., 2009), 1 line no change (Peng et al., 2009), and 2 lines showing increased levels (Burbach et al., 2004; Schulte-Herbrüggen et al., 2008; Szapacs et al., 2004). BDNF levels were reported to be increased in the APdE9 mouse line used in the present study. We are not aware of any study so far investigating TrkB receptor levels in transgenic AD mouse models.

The APPswe/PS1dE9 double transgenic (APdE9) mouse line is a widely used model of AD. These mice develop amyloid plaques in the cortex and hippocampus starting at 4 months of age (Garcia-Alloza et al., 2006), but memory impairment manifests only between 8 and 12 months of age (Minkeviciene et al., 2008; Savonenko et al., 2005). Thus these mice recapitulate the order of pathological events in AD patients (amyloid plaques develop gradually over years before memory impairment leads to the clinical diagnosis) as revealed by recent positron-emission tomography (PET) imaging studies with amyloid binding a ligand (Aizenstein et al., 2008; Kadir et al., 2012), in contrast to most other APP transgenic mice in which memory impairment usually precedes amyloid plaque formation (Van Dam et al., 2003; Westerman et al., 2002). This mouse line therefore offers an excellent model for studying molecular mechanisms downstream of amyloid plaque formation leading to memory impairment.

We have here investigated the role of TrkB signaling in amyloid-induced neuropathology leading to memory loss in the APdE9 mouse model of AD. We found that increased amyloid-beta (Aβ) peptide levels increase the expression of the truncated TrkB.T1 isoform in vitro in cultured neurons and in vivo in the brains of APdE9 mice. To further mimic impaired signaling through TrkB receptors as it occurs in AD, we cross-bred APdE9 mice with TrkB.T1 mice (Saarelainen et al., 2000a, 2000b), while crossing of APdE9 mice with those overexpressing the full-length TrkB.TK receptor (Koponen et al., 2004) was used to counteract the disturbed balance between truncated and full-length TrkB receptor. Importantly, all these mouse lines shared the same C57BL6/J background and had robust transgene expression in the cortex and hippocampus. Our results lend support to the idea that impaired TrkB signaling contributes to the memory impairment in AD.

2. Methods

2.1. Animals

The APPswe/PS1dE9 (APdE9) founder mice were obtained from Johns Hopkins University, Baltimore, MD, USA (D. Borchelt and J. Jankowsky, Dept. Pathology) and a colony was established at the University of Kuopio. These mice were generated by coinjection of chimeric mouse/human APPswe (mouse APP695 harboring a human Aβ domain and mutations K595N and M596L linked to Swedish familial AD pedigrees) and human PS1-dE9 (deletion of exon 9) vectors controlled by independent mouse prion protein promoter elements (Jankowsky et al., 2004). This line was originally maintained in a hybrid C3HeJ × C57BL6/J F1 background, but the mice used in the present study were derived from backcrossing to C57BL6/J for 12 generations.

The development of mice overexpressing the truncated TrkB (TrkB.T1) or the full-length TrkB (TrkB.TK) receptors specifically in neurons (≥ 2-fold overexpression throughout cortex and hippocampus) have been described previously by Saarelainen et al. (2000a, 2000b) and Koponen et al. (2004), respectively. Expression of the transgenic receptor in both the TrkB.T1 and TrkB.TK mouse lines is highest in the cerebral cortex and hippocampus (Koponen et al., 2004; Saarelainen et al., 2000a), thus overlapping with the brain areas with the highest amyloid load in the APdE9 mouse (Jankowsky et al., 2004). In addition, both TrkB transgenic lines have moderate transgene expression in the thalamus, and the TrkB.TK line also moderate expression in the amygdala and cerebellum (Koponen et al., 2004; Saarelainen et al., 2000a). These mouse lines were originally maintained in a hybrid BALB/c × DBA/2 background, but the mice used in the present study were derived from backcrossing to C57BL6/J for 10 generations.

The housing conditions (National Animal Center, Kuopio, Finland) were controlled (temperature 22 °C, light from 7:00–19:00; humidity 50%–60%), and fresh food and water were freely available. The experiments were conducted according to the Council of Europe (Directive 86/609) and Finnish guidelines, and approved by the State Provincial Office of Eastern Finland.

Table 1
Number of animals involved in behavioral testing by gender and genotype

Age (months)	Males				Females			
TrkB.T1	AwTw	AwT1	A+Tw	A+T1	AwTw	AwT1	A+Tw	A+T1
12	14	15	13	13	11	12	12	12
TrkB.TK	AwTw	AwTK	A+Tw	A+TK	AwTw	AwTK	A+Tw	A+TK
15	14	12	11	14	15	14	12	10

Codes for genotypes resulting from cross-breedings: APdE9 +/w × TrkB.T1 +/w breeding: AwTw = APdE9 w/w × TrkB.T1 w/w = double wild-type; AwT1 = APdE9 w/w × TrkB.T1 +/w = only TrkB.T1 transgenic; A+Tw = APdE9 +/w × TrkB.T1 w/w = only APdE9 transgenic; A+T1 = APdE9 +/w × TrkB.T1 +/w = double transgenic; APdE9 +/w × TrkB.TK +/w breeding: AwTw = APdE9 w/w × TrkB.TK w/w = double wild-type; AwTK = APdE9 w/w × TrkB.TK +/w = only TrkB.TK transgenic; A+Tw = APdE9 +/w × TrkB.TK w/w = only APdE9 transgenic; A+TK = APdE9 +/w × TrkB.TK +/w = double transgenic.
Key: +, transgene; w, wild type allele.

2.2. Behavioral testing

APdE9 × TrkB.T1 crossed mice underwent a neurological test battery at 12 months of age, while mice of the APdE9 × TrkB.TK crossing were tested at an older age, 15 months, based on the primary hypothesis that overexpression of the catalytic TrkB receptor would alleviate the neurological phenotype of APdE9 mice while overexpression of the truncated TrkB.T1 receptor would exacerbate the phenotype. Both males and females were included.

The number of animals and the abbreviations used for various genotypes in each test series and their genotypes are summarized in Table 1.

The Morris swim navigation task (water maze) was used to test spatial learning and memory. The apparatus was a black plastic pool with a diameter of 120 cm. A black escape platform (14 cm × 14 cm) was hidden 1.0 cm below the water surface. The temperature of the water was kept at 20 ± 0.5 °C throughout the experiment, and a 5- to 10-minute recovery period was allowed between the training trials. First, the mice were pretrained (2 days) to find and climb onto the submerged platform, aided by a guiding alley (1 m × 14 cm × 25 cm) leading to the platform. In the testing phase (days 1–4), five 60-second trials per day were conducted with a hidden platform. The platform location was kept constant and the starting position varied between 4 constant locations at the pool edge, with all mice starting from the same position in any single trial. Each mouse was placed in the water with its nose pointing towards the wall. If the mouse failed to find the escape platform within 60 seconds, it was placed on the platform for 10 seconds by the experimenter. On day 5 the trial length was set to 40 seconds. The last trial on that day was run without the platform to test the search bias. The experimenter marked the start and the end of each test using a remote controller. A computer connected to an image analyzer (HVS Image, Hampton, UK) calculated the escape latency (time between the start and the end), swim path length, and the swimming speed.

Thigmotaxis was assessed by dividing the pool into 3 concentric zones of equal surface area, and calculating the time spent in the outer zone. The search bias during the probe trial was measured by calculating the time the mice spent in the vicinity of the former platform position. We defined this as a target area, centered on the platform, with a diameter of 30 cm. This target area comprised 6.25% of the total surface, which means that a mouse swimming randomly in the pool would be expected to spend 3.75 seconds in the target area during the 60-second probe trial.

Spontaneous explorative activity was tested using an automated activity monitor (TruScan, Coulbourn Instruments, Whitehall, PA, USA) based on infrared photo detection. The system consisted of an observation cage with white plastic walls (26 × 26 × 39 cm) and 2 rings of photo detectors enabling separate monitoring of horizontal (XY-move time) and vertical activity (rearing). Males were tested first. The test cage was cleaned with 70% ethanol before each mouse to avoid odor traces. The test session took 10 minutes and was replicated after 48 hours to assess the extent of habituation to the test cage.

2.3. Histology

At the end of the experiment all male mice were deeply anesthetized with pentobarbiturate-chloral hydrate cocktail (60 mg/kg each) and perfused transcardially with 50 mL heparinized ice-cold 0.9% saline (10 mL/min) followed by 4% paraformaldehyde. Brains were transferred to a 30% sucrose solution overnight and finally stored in a cryoprotectant in −20 °C for later immunohistology. The brains were cut on a sliding/freezing microtome into 35-μm coronal sections and selected sections at the level of the septal half of the hippocampus stained for human amyloid-β selective antibody W02 (Genetics, Switzerland).

For T1 mice, 2 sections with a distance of 420 μm, and for TK mice, 3 sections with 210 μm between them (out of total 28 hippocampal sections) were selected from the septal half of the hippocampus. The sections were photographed using the Olympus BX40 microscope (Tokyo, Japan) with DP50 camera attached and images were treated and analyzed using Photoshop CS3 program (Adobe Systems Inc., San Jose, CA, USA). The images were transformed to grayscale and their brightness and contrast was changed using the shadow-highlight command (3 times for T1 and 1 time for TK, maintaining the same threshold for all subgroups in a series). The area of the hippocampus was measured using the lasso-tool and hippocampal amyloid plaques

were measured using the color range command (using threshold 200 for T1 and 140 for TK). The final value was obtained by dividing the amyloid plaque area by the total hippocampal area.

2.4. Analysis of TrkB receptor levels in vitro and in vivo

2.4.1. Neuronal culture

Neurons were isolated from fetuses of 18-day pregnant Sprague-Dawley rats (Harlan Interfauna Iberica, SL, Barcelona, Spain), as described previously (Brewer et al., 1993). The animals were handled according to European Union guidelines and Portuguese law on Animal Care, and anesthetized with halothane before decapitation. The fetuses were collected in Hanks' balanced salt solution (HBSS-1, Gibco, Paisley, UK), the cerebral cortex (in cortical cultures) or the hippocampus (in hippocampal cultures) were mechanically fragmented, and the fragments transferred to a 0.025% (wt/vol) trypsin in HBSS without Ca^{2+} and Mg^{2+} (HBSS-2, Gibco) solution and incubated for 15 minutes at 37 °C. After trypsinization, cells were washed twice in HBSS-2 containing 10% (vol/vol) fetal bovine serum, and resuspended in Neurobasal medium (Gibco) supplemented with 0.5 mM L-glutamine, 25 μM L-glutamic acid, 2% B-27 supplement (Gibco), and 2 U/mL PenStrep (Sigma, Steinheim, Germany). Cells were cultured at a plating density of 6×10^4 cells/cm^2 on poly-$_D$-lysine coated plastic dishes and maintained at 37 °C in a humidified atmosphere of 5% CO_2. At 4 days in vitro (DIV) half of medium was changed by medium without L-glutamic acid. In experiments with pure neuronal cultures, the antimitotic drug 5-fluouraucil was added to medium during 4–7 DIV. Incubations with A$\beta_{25–35}$ peptide (Bachem, Bubendorf, Switzerland) or with A$\beta_{1–42}$ (rPeptide, Bogart, GA, USA) were performed at 7 DIV (from stock solutions of 1 mg/mL in Mili-Q water for both peptides).

2.4.2. Thioflavin T binding

The presence of fibrillary Aβ species was confirmed by thioflavin T (ThT) binding assay (Nilsson, 2004). Briefly, ThT was incubated at a final concentration of 20 μM with 3 μM of A$\beta_{1–42}$ and A$\beta_{25–35}$ species in 50 mM Tris-HCl pH 7.4. Emission wavelength scan was performed with an excitation wavelength of 450 nm using a plate reader (Tecan Infinite 200, Mannendorf, Switzerland) with the typical 490-nm maximum emission wavelength.

2.4.3. Atomic force microscopy

Atomic force microscopy (AFM) was used to characterize the morphology of A$\beta_{1–42}$ and A$\beta_{25–35}$ species. Samples for AFM were prepared as follows: 10 μL of protein sample at a concentration of 30 μM was applied on a freshly cleaved mica substrate previously glued to a glass coverslip and allowed to adsorb for 5 minutes. Unbound protein was rinsed 5 times with 10 μL Mili-Q water (resistivity $>$ 18 MW cm) 0.22 mm filtered. The sample was then mounted on the AFM stage in 60 μL of Mili-Q water.

AFM imaging was performed with uncoated silicon nitride cantilevers OMCL-TR800PSA-1 from Olympus with a typical stiffness of 0.57 N/m for intermittent contact mode. The scan rate was set to less than 1 Hz and the force applied on the sample was maintained at the lowest possible value by continuously adjusting the set point and gain during the imaging. The cantilever oscillation was turned to a frequency of 15–20 kHz. Height and error signals were collected and images were line-fitted as required. Tip artifacts were ruled out by image analysis. All AFM images have 512×512 pixels and acquired at a typical scan speed of 0.7 mm/s.

2.4.4. Analysis of TrkB receptor levels in neuronal cultures

Sodium dodecyl sulfate polyacrylamide gel electrophoresis (SDS-PAGE) was used to determine the density of TrkB immunolabeling. Briefly, after washing once with ice-cold phosphate-buffered saline (PBS), cells were lysed on ice in a lysis buffer containing (in mM): 50 Tris-HCl (pH 7.5), 150 NaCl, 5 ethylenediamine tetra-acetic acid (EDTA), 1% NP-40 and 1× protease inhibitor mixture (Roche, Penzberg, Germany). Cell lysates were clarified by centrifugation, and an equal amount of protein for each sample (40 μg) was separated on 10% SDS-polyacrylamide electrophoresis gels, and then transferred onto nitrocellulose membranes. After blocking with a 5% nonfat dry milk solution, the membranes were incubated (overnight at 4 °C) with primary antibodies against TrkB receptors (BD Biosciences, San Jose, CA, USA) and α-tubulin (Abcam, Cambridge, UK), and then with horseradish peroxidise (HRP)-conjugated secondary antibodies (Santa Cruz, Heidelberg, Germany) for 1 hour at room temperature. Finally, the membranes were developed using ECL-plus (Amersham Biosciences, Buckinghmashire, UK) and bands were quantified by digital densitometry (ImageJ 1.45 software). α-tubulin was used as a loading control.

2.4.5. Cell death evaluation

Global cell death was evaluated by the lactate dehydrogenase (LDH) assay (Sigma, Steinheim, Germany) according to the manufacturer's instructions and using 120 μL of the incubation medium. To specifically evaluate the degree of cell death induced by apoptosis, caspase-3 activation was measured in 50 μg of total protein from cell lysates. General caspase-3-like activity was evaluated by enzymatic cleavage of p-nitroanilide chromophore (pNA) from the substrate N-acetyl-Asp-Glu-Val-Asp (DEVD) pNA (Sigma). The proteolytic reaction was preceded in lysis buffer containing 50 μM DEVD-pNA (Sigma). The reaction mixtures were incubated at 37 °C for 1 hour, and the release of pNA was determined by measuring absorbance at 405 nm using a 96-well plate reader.

2.4.6. Brain tissue samples

At the end of the experiment all female mice (12 months) and a separate group of 3- and 14-month-old APdE9 ($n = 6$

per age) and 6 wild type ($n = 6$ per age) male mice were deeply anesthetized with pentobarbiturate-chloral hydrate cocktail (60 mg/kg each) and perfused transcardially with 50 mL heparinized ice-cold 0.9% saline (10 mL/minute). Brains were then removed and dissected on ice into frontal cortex, parietal cortex, and hippocampus (bilateral). The brain blocks were snap-frozen in liquid nitrogen and stored at −70 °C for biochemical assays. The protein levels of full-length TrkB and truncated TrkB.T1 were analyzed from raw lysate samples with Western blotting as described earlier (Saarelainen et al., 2003; Rantamäki et al., 2007). Briefly, equal amount of protein were loaded and separated in 7.5% SDS-PAGE. Next the proteins were blotted onto polyvinylidene fluoride (PVDF) membrane (300 mA, 1 hour, 4 °C), membranes blocked with 5% nonfat dry milk (in Tris-buffered saline [TBS] + 0.1% Tween (TBST); 1 hour, room temperature) and incubated overnight at 4 °C with an antibody directed against the extracellular portion of TrkB (1:1000 in blocking solution; BD Biosciences, Franklin Lakes, NJ, USA). The next morning, membranes were washed with TBST and incubated with horseradish peroxidase conjugated secondary antibody (1:10,000 in blocking solution, 1 hour, room temperature, BioRad Laboratories, Hercules, CA, USA). After subsequent TBST washes, secondary antibodies were visualized using electrochemiluminescence kit (ECL+; GE Healthcare, Piscataway, NJ, USA) followed by an exposure to Fuji LAS-3000 camera (Tamro, Vantaa, Finland). For loading and normalization control the membranes were incubated with Ponceau S solution (0.01% [wt/vol] Ponceau S, 5% acetic acid [vol/vol]) to visualize proteins. The mRNA levels of TrkB.TK and TrkB.T1 were analyzed with real time-polymerase chain reaction (PCR) as described in Karpova et al. (2009).

2.5. Phosphoprotein analysis

The dissected brain blocks of 12-month-old female mice were used for the phosphoprotein assay (8 animals for each genotype). In these animals, the hippocampus was further dissected into CA1, CA3, and dentate gyrus (DG) samples. The samples were snap-frozen in liquid nitrogen and stored at −70 °C. Frozen tissue was lysed at 4 °C (20 seconds, 5000 rpm) in a solubilization buffer (10 mM Tris-Cl, 50 mM NaCl, 1% Triton X-100, 30 mM sodium pyrophosphate, 50 mM NaF, 5 mM ZnCl2, 100 mM Na_3VO_4, 1 mM dithiothreitol (DTT), 5 nM okadaic acid and Complete antiprotease mix (1 tab/10 mL; Roche) using an automated sample lyzer (Precellys, Bertin Technologies, France). Homogenates were kept on ice for 30 minutes and insoluble material removed by centrifugation (13,000 rpm for 15 minutes at 4 °C). Total protein quantification was assessed by bicinchoninic acid (BCA) assay against a standard of bovine serum albumin (1, 2, 5, 10, 15, 20, and 30 $\mu g/\mu L$) using a Bio-Rad BCA reagent. Sample optical density was measured in a plaque spectrophotometer at 594 nm. Samples were then equalized in the solubilization buffer and denatured in 2× Laemmli's loading buffer by boiling samples at 95 °C for 5 minutes. Denatured samples (30 μg) were then separated on SDS-PAGE gels (8% to 12%) and transferred onto nitrocellulose membrane.

Blots were saturated 1 hour in TRIS-buffered saline [Euromedex] + 0.1% Tween 20 (TBS-T) containing 5% low fat dry milk (Bio-Rad). After 3 washes in TBS-T (5 minutes) blots were incubated (4 °C, overnight) with primary antibodies in 5% bovien serum albumin (BSA) TBS-T (see Supplementary Table 1 for the list of antibodies and dilutions). The second day blots were washed 3 times in TBS-T (10 minutes) and incubated (1 hour, room temperature) with the secondary antibodies diluted (see supplementary Table 1) in 5% low fat dry milk TBS-T. After 3 washes in TBS-T (10 minutes), membranes were exposed to ECL or ECL+ reagent and then exposed to photographic film (GE Healthcare). Films were processed by hand. When needed, membranes were stripped of antibodies (10-minute incubation in Reblot strong solution [Millipore]), washed twice in TBS-T and reprocessed with another antibody. Phosphorylated forms of proteins were always probed first, followed by the total protein. The efficacy of the stripping step was assessed by omitting the first antibody and verifying the lack of signals on the blot. Films were imaged using a charge-coupled device (CCD) camera and optical density of the bands was quantified using Genetools analysis software (Syngene). Optical density values for total proteins were normalized to β-actin whereas phosphoproteins were normalized to total protein.

2.6. Statistics

The effect of Aβ incubation on TrkB receptor density in neuronal cultures and the comparison between APdE9 versus wild type mice was done with Student t test. For multiple comparisons, statistical significance was assessed by the 1-way analysis of variance (ANOVA) with Bonferroni's correction. The statistical analysis of behavioral test was done using SPSS for Windows 14.0 software (SPSS Inc., Chicago, IL, USA). The normal distribution of values for selected parameters in separate groups was tested using Kolmogorov-Smirnov Z 1-sample test. The main means of analysis was 2-way ANOVA with APdE9 (transgenic A+ vs. wild type Aw) and TrkB (full-length TK or dominant negative T1 vs. wild type Tw) as between subjects factors. When several time points were included as a within-subject factor, ANOVA for repeated measures was used with the same A and T factors. The impact of APdE9 genotype to the studied parameter was assessed by comparing AwTw versus A+Tw groups with Student t test. Post hoc analyses were done using Dunnett's test with the AwTw groups as the reference. Statistical significance was set at $p < 0.05$.

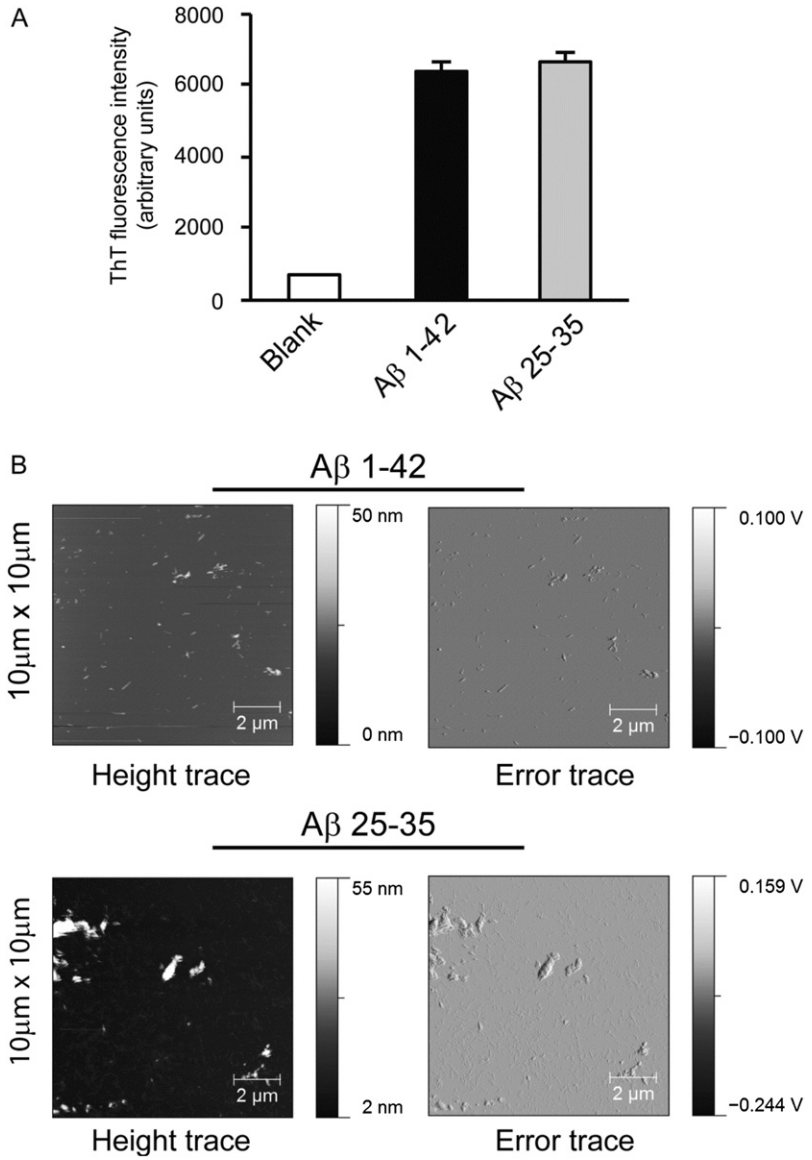

Fig. 1. Amyloid beta $(A\beta)_{1-42}$ and $A\beta_{25-35}$ peptides have fibrillary structures. (A) Thioflavin T (ThT) fluorescence assay with excitation and emission wavelengths of 450 nm and 490 nm, respectively. Both peptides interacted with ThT, indicating increased β-sheet structure, typical of amyloid-like fibrillar species. (B) Atomic force microscopy (AFM) analysis of the $A\beta_{1-42}$ and $A\beta_{25-35}$ peptides. Both peptides appear as heterogeneous population with both protofibrillar and fibrillar structures (scale bar 2 μm).

3. Results

3.1. $A\beta_{1-42}$ and $A\beta_{25-35}$ peptides show fibrillary structures

To analyze the structural properties of the different species applied to neuronal cultures in the study, we performed both ThT binding assays and AFM. Both $A\beta_{1-42}$ and $A\beta_{25-35}$ peptides showed a ThT emission wavelength shift followed by a fluorescence intensity enhancement, typical of β-sheet amyloid structures interaction (Fig. 1A). By AFM the $A\beta_{1-42}$ and $A\beta_{25-35}$ peptides show similar structures as a heterogeneous population exhibiting protofibrillar and fibrillar ones (Fig. 1B).

3.2. Aβ increases truncated TrkB levels in vitro

Because decreased full-length TrkB (TrkB.TK) and increased truncated TrkB receptor levels have been reported in AD brain, we hypothesized that amyloid-beta peptide (Aβ), by itself, might induce similar changes in TrkB receptor isoforms. To test this hypothesis, cortical and hippocampal cells were cultured for 7 DIV, treated with Aβ peptides and TrkB receptor immunoreactivity was evaluated by Western blotting.

Incubation of cortical cells with $A\beta_{25-35}$ (25 μM) (as described in Rodrigues et al., 2000) induced a dramatic increase in truncated TrkB receptor levels compared with

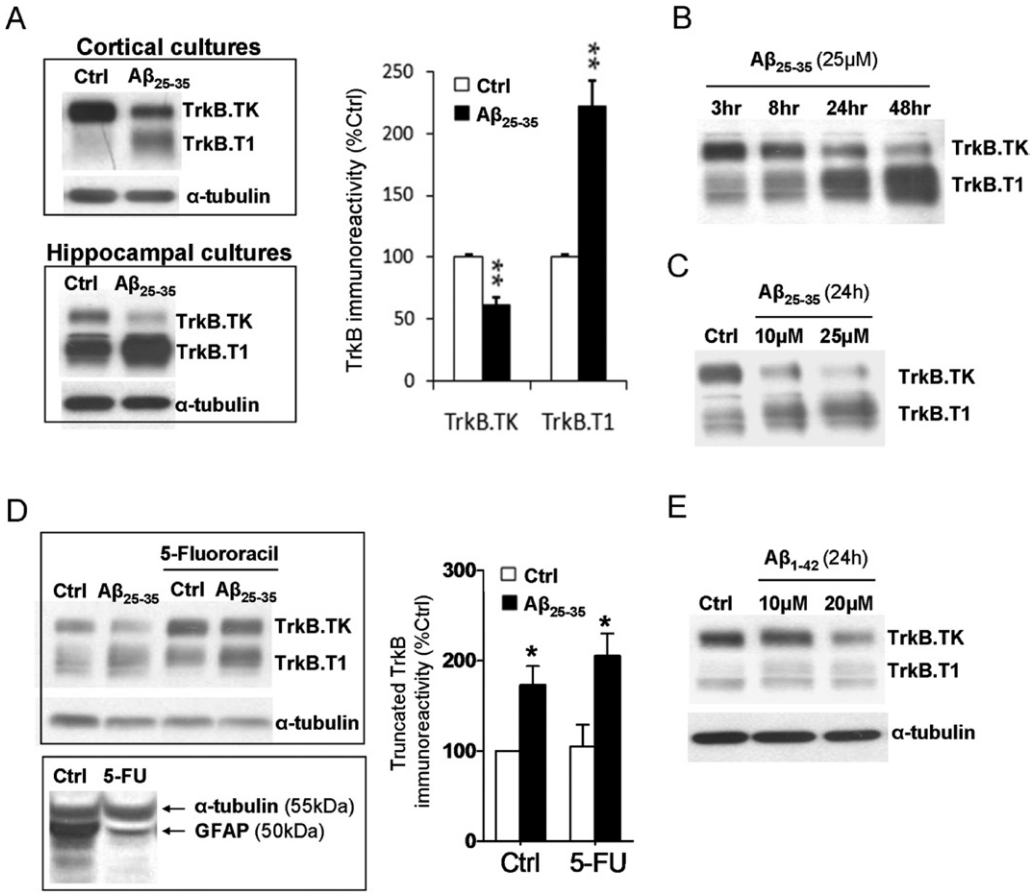

Fig. 2. Effect of amyloid beta (Aβ) peptide exposure on truncated and full-length TrkB receptor levels. (A) Primary cultures of cortical cells (upper left panel) and hippocampal cells (lower left panel) were incubated at 7 days in vitro (DIV) with Aβ_{25-35} (25 μM) for 24 hours and levels of full-length (TrkB.TK) and truncated TrkB (TrkB.T1) were determined by Western blotting. Average data from 8 independent cortical cultures is shown in right panel (** $p < 0.01$ compared with control [Ctrl], Student t test). (B) Time-dependent changes in TrkB.TK and TrkB.T1 densities after 3, 8, 24, and 48 hours of incubation of 7 DIV cortical cultures with Aβ_{25-35} (25 μM). (C) Dose-dependent changes in TrkB.TK and TrkB.T1 levels after 24 hours of incubation of 7 DIV cortical cultures with Aβ_{25-35}. (D) Comparison of the influence of Aβ_{25-35} (25 μM) exposure in nontreated cortical cultures and in cultures treated with 5-fluorouracil (5-FU) (upper left panel), to markedly decrease glial cells number as confirmed by glial fibrillary acidic protein levels (GFAP) (lower left panel). Average effect of Aβ_{25-35} (25 μM) on truncated TrkB levels in 3 independent cultures; both conditions were shown in the right panel (* $p < 0.05$ as compared with nontreated control, Student t test). (E) Dose-dependent changes on TrkB.TK and TrkB.T1 levels on 7 DIV cortical cultures exposed for 24 hours to Aβ_{1-42} peptide.

control cells (100 ± 2.3% vs. 223 ± 19.9%; $n = 8$, $p < 0.01$, Student t test; Fig. 2A, upper left and right panels), whereas the levels of TrkB.TK receptors were decreased (100 ± 1.7% vs. 61 ± 6.3%; $n = 8$; $p < 0.01$, Student t test; Fig. 2A, upper left and right panels). The same pattern of alteration in TrkB receptor isoforms was also observed in hippocampal cultures (Fig. 2A, lower left panel). The effects of Aβ_{25-35} exposure on TrkB receptors were time and concentration-dependent (Fig. 2B and C), so that longer incubation times with Aβ or higher concentrations of Aβ produced a more robust change on TrkB isoforms levels.

Because glial cells are enriched in truncated TrkB.T1 isoform (Rose et al., 2003), we tested the effect of the Aβ_{25-35} peptide on truncated TrkB in neuronal cultures previously treated with the antimitotic drug 5-fluorouracil (5-FU). Despite the marked reduction in the astrocytic marker, the glial fibrillary acidic protein (GFAP), observed in the cultures treated with 5-FU (Fig. 2D, lower left panel), Aβ_{25-35} treatment still increased truncated TrkB receptor levels in a magnitude similar to that observed in cells from the same culture but not treated with 5-FU (Fig. 2D, right panel).

Aβ_{1-42} (10–20 μM for 24 hours), the most frequent Aβ peptide in AD, also produced a concentration-dependent increase (approximately 28% for 20 μM) of the truncated TrkB and a concentration-dependent decrease (approximately 40% for 20 μM) in TrkB.TK levels in cortical cultures (7 DIV) (Fig. 2E). Therefore, our data suggest that Aβ peptide simultaneously increases the levels of the truncated TrkB receptors and decreases levels of the full-length TrkB receptors in primary neuronal cultures, producing a pattern of alterations similar to that reported in the brain of AD patients.

Moderate cell death is expected to occur after Aβ peptide incubation. Indeed, 24 hours after incubating the

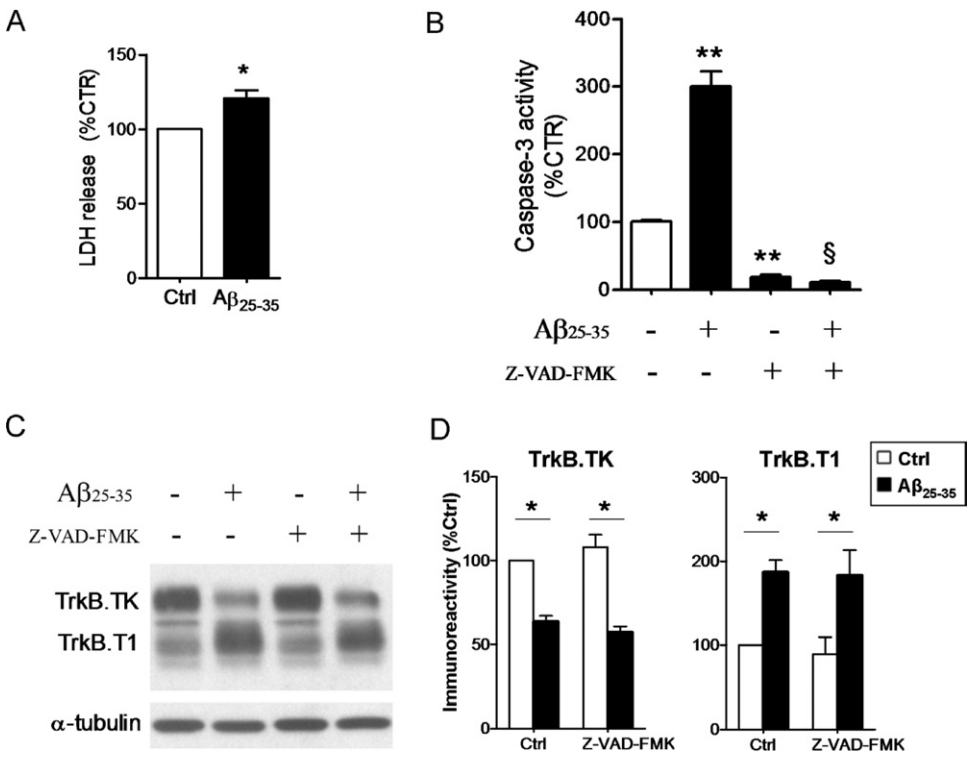

Fig. 3. Amyloid beta-induced increase in TrkB.T1 and decrease in TrkB.TK levels still occur when Aβ-induced cell death by apoptosis is inhibited. (A) Primary cultures of cortical cells were incubated at 7 days in vitro (DIV) with $A\beta_{25-35}$ (25 μM) for 24 hours, after which the levels of released lactate dehydrogenase (LDH) were measured. Average data from 6 independent cortical cultures are presented (* $p < 0.05$ compared with control [Ctrl], Student *t* test). (B) Caspase-3-like activity of cell lysates measured after 24 hours of $A\beta_{25-35}$ (25 μM) incubation of 7 DIV cortical cultures, in the presence and absence of the pan-caspase inhibitor Z-VAD(OMe)-FMK (20 μM) (** $p < 0.01$ compared with control [Ctrl]; § $p < 0.01$ compared with $A\beta_{25-35}$ alone; analysis of variance [ANOVA] with Bonferroni's correction). (C) Representative Western blot image of TrkB.TK and TrkB.T1 levels detected in neuronal cultures from 7 DIV with $A\beta_{25-35}$ (25 μM) in presence or absence of Z-VAD(OMe)-FMK (20 μM). (D) Average data from densitometric quantification of TrkB.TK (left) and TrkB.T1 (right) immunoreactivity (C) of 4 independent cortical cultures (* $p < 0.05$, Student *t* test).

neurons with $A\beta_{25-35}$ (25 μM) there was an increase Fig. 2A, (21 ± 5%, $p < 0.05$, $n = 6$) in activity of LDH, a soluble cytosolic enzyme that is released following loss of membrane integrity resulting from either apoptosis or necrosis (Bonfoco et al., 1995), into incubation medium. The intracellular caspase-3 activity, a central effector of apoptotic cell death, was even more markedly increased (a 3-fold increase, Fig. 3B, $p < 0.01$, $n = 4$). However, the cell-permeant pan-caspase inhibitor, (Z-VAD(OMe)-FMK), known to inhibit apoptotic cell death (Slee et al., 1996), failed to influence the $A\beta_{25-35}$ (25 μM) induced increase in TrkB.T1 and decrease in TrkB.TK levels (Fig. 3C and D, $p < 0.05$, $n = 4$), while it fully blocked the $A\beta_{25-35}$ (25 μM)-induced enhancement of caspase-3 activity (Fig. 3B, $p < 0.01$, $n = 4$). These results suggest that the Aβ-induced alterations on TrkB receptors are not a direct consequence of apoptotic cellular death.

3.3. The expression of cortical TrkB.T1 receptors in APdE9 mice increases with age and amyloid load

We next investigated whether increased Aβ levels might influence the expression of TrkB isoforms in brain in vivo. To this end, we investigated the expression of TrkB isoforms in the brains of APdE9 mice at different ages. At the age of 3 months, when no amyloid plaques are yet present, the expression levels of TrkB isoforms were the same as those in wild type mice (Fig. 4A). However, at the age of 12–14 months, when there is abundant amyloid load in the cortical regions of APdE9 mice, the levels of the truncated TrkB.T1 isoform were significantly increased in several cortical regions, most pronounced in the frontal cortex (Fig. 4B), but not in the hippocampus (Table 2). The levels of the full-length TrkB.TK isoform were also somewhat increased, and the increase reached a statistically significant level in the parietal cortex (Table 2). Nevertheless, the ratio of TrkB.TK over TrkB.T1 was significantly decreased in the frontal cortex and there was a trend toward lower values in other cortical regions, too, indicating that there is a more substantial increase in the truncated T1 isoform when compared with the TrkB.TK isoform. Consistent with this, the expression of TrkB.T1 mRNA, but not of TrkB.TK mRNA was significantly upregulated in the parietal cortex of aged female APdE9 mice compared with controls (TrkB.T1: 100.0 ± 9.1% vs. 132.3 ± 9.7%; TrkB.TK: 100.0 ± 5.4% vs. 103.5 ± 8.7%; Student *t* test). These data suggest that the upregulation of cortical TrkB.T1 expression in APdE9

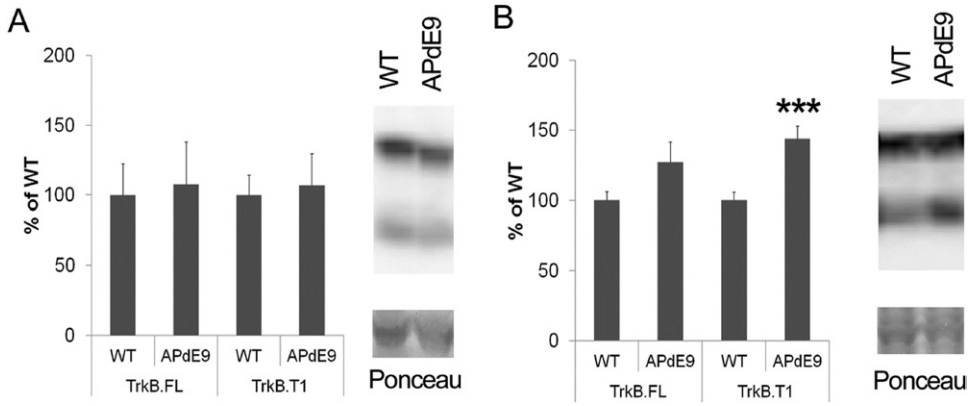

Fig. 4. (A) The protein levels of full-length TrkB and truncated TrkB.T1 receptors in the frontal cortex of APPswe/PS1dE9 (APdE9) male mice are comparable to their wild type (WT) control mice at the age of 3 months when no amyloid plaques are yet present, but significantly upregulated in the aged (14 months); (B) APdE9 mice with substantial amyloid load in the cortex. Immunoreactivity normalized with Ponceau staining. Group means + standard error of the mean (SEM) are shown. *** $p < 0.005$, Student t test.

mice was only evident in aged animals already showing prominent Aβ plaques and memory impairment, whereas at 3 months of age no significant changes in TrkB receptor levels were observed.

3.4. TrkB.T1 and TrkB.TK overexpression have different impact on signaling pathways downstream of the TrkB receptor

To assess the functional significance of the changes we observed in TrkB.T1 and TrkB.TK levels, we analyzed protein and phosphoprotein levels of mediators of the main signaling pathways downstream of the TrkB receptor, namely the phosphoinositol kinase 3 (PI3K) and extracellularly regulated kinase (ERK) signaling pathways. Results from cortical and hippocampal (DG) samples are summarized in Table 3. As expected TrkB.T1 overexpression alone decreased TrkB signaling, which is most clearly seen as suppression of Akt (protein kinase B) and glycogen synthase kinase 3β (GSK-3β) activity (measured as the ratio between the active, phosphorylated form and the total levels of the corresponding protein). On the other hand, the effect of TrkB.TK overexpression was modest, and only having significant inhibitory effect on cyclic adenosine monophosphate response element-binding protein (CREB) phosphorylation. A complicating factor in this signaling pathway analysis is that APdE9 transgene itself increased both GSK-3β and CREB phosphorylation, so that both TrkB.T1 and TrkB.TK overexpression partially opposed the APdE9 effect and may account for the modest effects observed (see Table 3).

Table 2
Levels of TrkB receptors in 12-month-old female APdE9 mouse brains

	WT	APdE9	p-value
Hippocampus			
TrkB.TK	100.0 ± 4.1%	106.1 ± 9.1%	0.55
TrkB.T1	100.0 ± 12.3%	92.6 ± 7.6%	0.61
TrkB.FL/TrkB.T1	1.2 ± 0.2	1.2 ± 0.2	0.89
Frontal cortex			
TrkB.TK	100.0 ± 2.8%	107.6 ± 6.0%	0.26
TrkB.T1	100.0 ± 8.9%	157.1 ± 15.4%**	0.004
TrkB.FL/TrkB.T1	1.1 ± 0.1	0.8 ± 0.1*	0.016
Parietal cortex			
TrkB.TK	100.0 ± 4.9%	118.6 ± 7.5%*	0.049
TrkB.T1	100.0 ± 7.2%	143.3 ± 17.8%*	0.034
TrkB.FL/TrkB.T1	1.0 ± 0.1	0.9 ± 0.1	0.38

Group means + standard error of the mean (SEMs) are shown.
Key: +, transgene; w, wild type allele.
* $p < 0.05$, ** $p < 0.01$, Student t test.

3.5. Overexpression of full-length versus truncated TrkB receptors has opposite effects on spatial learning and memory in APdE9 mice

To investigate the effects of the expression of different TrkB isoforms on the behavioral phenotype of the APdE9 mice, we crossed these mice with transgenic mice overexpressing the TrkB.T1 (Saarelainen et al., 2000a, 2000b) or the TrkB.TK isoform (Koponen et al., 2004) in adult neurons. The cross-breeding resulted in 4 possible genotypes that were coded as follows: APdE9 +/w × TrkB.T1 +/w breeding: AwTw, AwT1, A+Tw, A+T1; APdE9 +/w × TrkB.TK +/w breeding: AwTw, AwTK, A+Tw, A+TK (where w stands for wild type allele and A+, T1, and TK for mice heterozygous for the respective transgene, see Table 1 for details).

We have used Morris swim task to investigate the effects of TrkB modulation on the spatial memory impairment in the APdE9 mice. At 12 months of age, APdE9 male mice showed a robust impairment in escape latency to the hidden platform ($F(1,52) = 23.1$, $p < 0.001$; Fig. 5A). TrkB.T1 overexpression alone had no effect on the escape latency ($p = 0.26$) (Fig. 5A). However, double transgenic A+T1 mice performed the worst (Fig. 5A), suggesting that the overexpression of a dominant-negative TrkB aggravates the memory impairment in APdE9 mice. Similarly, among females, A+T1 mice were the most impaired group but no main

Table 3
Protein levels of main signaling peptides associated with the TrkB receptors given as percentage relative to the double wild type (AwTw) group means

Parietal cortex	AwTw (n = 8)	AwT1 (n = 5)	A+Tw (n = 8)	A+T1 (n = 8)	ANOVA
Akt_act	1 ± 0.02	0.85 ± 0.03[a]	0.95 ± 0.04	0.94 ± 0.03[a]	TrkB.T1[a]
pAkt_tot	1 ± 0.03	0.92 ± 0.02	1.04 ± 0.08	0.98 ± 0.05	
GSK3β_act	1 ± 0.06	0.92 ± 0.03	0.92 ± 0.03	0.96 ± 0.05	
pGSK3β_tot	1 ± 0.09	0.86 ± 0.06[a]	1.16 ± 0.07[b]	0.93 ± 0.09[a,b]	APdE9[b], TrkB.T1[a]
ERK1_act	1 ± 0.05	0.77 ± 0.02	0.99 ± 0.07	0.96 ± 0.05	
pERK1_tot	1 ± 0.04	1.16 ± 0.07	1.15 ± 0.09	1.02 ± 0.04	
ERK2_act	1 ± 0.05	0.86 ± 0.06[a]	0.99 ± 0.05	0.93 ± 0.03[a]	TrkB.T1[a]
pERK2_tot	1 ± 0.04	1.07 ± 0.06	1.08 ± 0.10	1.21 ± 0.10	
CREB_act	1 ± 0.06	0.81 ± 0.05	0.91 ± 0.08	0.80 ± 0.09	
pCREB_tot	1 ± 0.09	1.19 ± 0.04	1.11 ± 0.13	1.08 ± 0.14	
Parietal cortex	AwTw (n = 7)	AwTK (n = 6)	A+Tw (n = 5)	A+TK (n = 6)	ANOVA
Akt_act	1 ± 0.04	0.98 ± 0.03	0.96 ± 0.04	1.01 ± 0.03	
pAkt_tot	1 ± 0.06	0.84 ± 0.07	1.03 ± 0.10	1.01 ± 0.09	
GSK3β_act	1 ± 0.03	0.98 ± 0.03	0.94 ± 0.03	0.98 ± 0.06	
pGSK3β_tot	1 ± 0.11	0.87 ± 0.14	1.08 ± 0.16	0.78 ± 0.08	
ERK1_act	1 ± 0.06	0.90 ± 0.04	1.05 ± 0.06	1.00 ± 0.10	
pERK1_tot	1 ± 0.12	0.74 ± 0.09	0.96 ± 0.11	0.94 ± 0.08	
ERK2_act	1 ± 0.04	0.94 ± 0.04	1.07 ± 0.04	1.08 ± 0.08	
pERK2_tot	1 ± 0.12	0.77 ± 0.08	0.96 ± 0.10	0.89 ± 0.13	
CREB_act	1 ± 0.05	1.05 ± 0.04	0.98 ± 0.07	0.88 ± 0.04	
pCREB_tot	1 ± 0.10	0.82 ± 0.09[a]	1.51 ± 0.20[b]	1.01 ± 0.15[a,b]	APdE9[b], TrkB.TK[a]
Dentate gyrus	AwTw (n = 5)	AwT1 (n = 5)	A+Tw (n = 6)	A+T1 (n = 7)	ANOVA
Akt_act	1 ± 0.00	0.75 ± 0.06[a]	0.88 ± 0.05	0.84 ± 0.07[a]	TrkB.T1
pAkt_tot	1 ± 0.04	0.92 ± 0.05[a]	1.04 ± 0.05	0.92 ± 0.05[a]	TrkB.T1
GSK3β_act	1 ± 0.06	0.89 ± 0.03[a]	0.89 ± 0.04	0.82 ± 0.04[a]	TrkB.T1
pGSK3β_tot	1 ± 0.08	0.86 ± 0.07	0.80 ± 0.09	0.77 ± 0.08	
ERK1_act	1 ± 0.10	0.97 ± 0.11	0.95 ± 0.08	0.92 ± 0.12	
pERK1_tot	1 ± 0.07	1.04 ± 0.13	0.98 ± 0.07	0.94 ± 0.08	
ERK2_act	1 ± 0.12	0.83 ± 0.06	0.93 ± 0.05	1.01 ± 0.05	
pERK2_tot	1 ± 0.10	1.13 ± 0.16	1.16 ± 0.15	1.39 ± 0.14	

Parietal cortical samples were analyzed for all mice while dentate gyrus samples were analyzed only in APdE9 × TrkB.T1 mice. Total protein levels are given relative to β-actin (act) while phospholyrated protein levels are given relative to the total protein (tot). Group mean ± standard error of the mean (SEM) are shown. See Table 1 for group genetic codes. The analysis of variance (ANOVA) column denotes significant main genotype effects at the significance levels of $p < 0.05$. There were no interactions between the genotypes.
Key: Akt = protein kinase B; GSK3β = glycogen synthase kinase 3β; ERK = extracellularly regulated kinase; CREB = cyclic adenosine monophosphate response element-binding protein; pAkt , pGSK3, pERK, pCREB: p = phospho; act = actin.
[a] Main effect of TrkB (T1 or TK vs. Tw).
[b] Main effect of APdE9 (A+ vs. Aw).

effects of either APdE9 ($F(1,45) = 1.0$, $p = 0.32$) or TrkB.T1 ($p = 0.40$) came out in the statistical analysis due to large within-group variation (Fig. 5B).

Analysis of escape latency was complicated by the fact that A+ male mice swam more slowly than Aw mice ($F(1,52) = 7.6$, $p = 0.008$). Therefore we also analyzed the total path length. The APdE9 genotype was also associated with a substantially increased path length in both males ($F(1,52) = 13.3$, $p = 0.001$) and females ($F(1,45) = 4.1$, $p < 0.05$), whereas TrkB.T1 had no main effect ($p > 0.79$). Again, the double transgenic A+T1 mice showed the worst performance of all groups (Fig. 5C and D). One essential component of successful performance in the Morris swim task for mice is to avoid developing a thigmotaxic strategy. Both male ($F(1,52) = 27.6$, $p < 0.001$) and female ($F(1,45) = 7.5$, $p = 0.009$) A+ mice spent more time in the wall zone than did Aw mice, and, although TrkB.T1 overexpression had no main effect by itself ($p > 0.34$), but the A+T1 mice showed the most persistent thigmotaxic behavior (Fig. 5E and F).

Spatial memory was assessed at the end of the test by a probe trial without the platform and both male ($F(1,52) = 8.7$, $p = 0.005$) and female ($F(1,45) = 4.9$, $p = 0.03$) A+ mice showed a weaker search bias than corresponding Aw mice, while TrkB.T1 overexpression alone had no effect ($p > 0.39$; Fig. 5G and H).

We next investigated the effect of neuronal overexpression of the full-length TrkB on the spatial memory deficits in the APdE9 mice. As we hypothesized that the TrkB.TK overexpression might ameliorate the behavioral deficits of the APdE9 mice, they were tested at the age of 15 months, when the memory impairment is fully evident. Indeed, at 15 months these mice showed a robust spatial learning impairment. Both male ($F(1,46) = 17.6$, $p < 0.001$) and female ($F(1,45) = 8.3$, $p = 0.006$) A+ mice had increased escape latencies compared with Aw mice

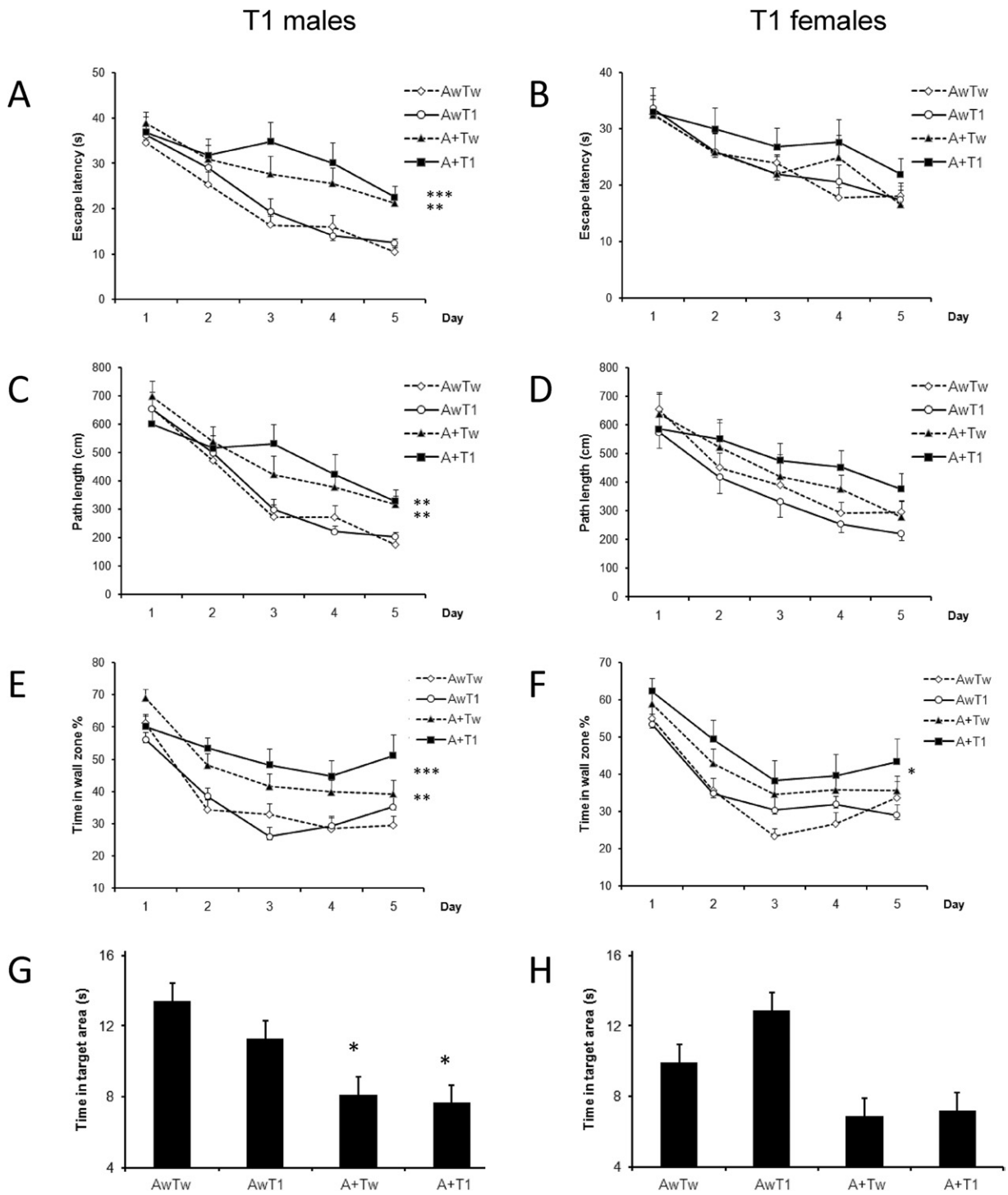

Fig. 5. Morris swim task in APdE9 × TrkB.T1 mice at 12 months of age. (A) Escape latency for males; and (B) females. (C) Swim path length for males; and (D) females. (E) Time spent in the zone close to the pool wall (% time) for males; and (F) females. (G) Time spent in the near vicinity of the former platform location during the probe test at the end of Day 5, for males; and (H) females. Group means + standard error of the mean (SEM) are shown. * $p < 0.05$, ** $p < 0.01$, *** $p < 0.001$, post hoc Dunnett's test compared with AwTw controls.

(Fig. 6A and B). TrkB.TK overexpression tended to decrease escape latencies in both genders (Fig. 6A and B). Among males, the effect did not reach significance ($p > 0.07$), but was significant among females ($F(1,45) = 4.6$, $p = 0.04$). In addition, there was a significant interaction between APdE9 and TrkB.TK genotypes ($F(1,45) = 4.3$, $p = 0.04$) among females. This was due to the fact that double transgenic A+TK mice had shorter escape latencies

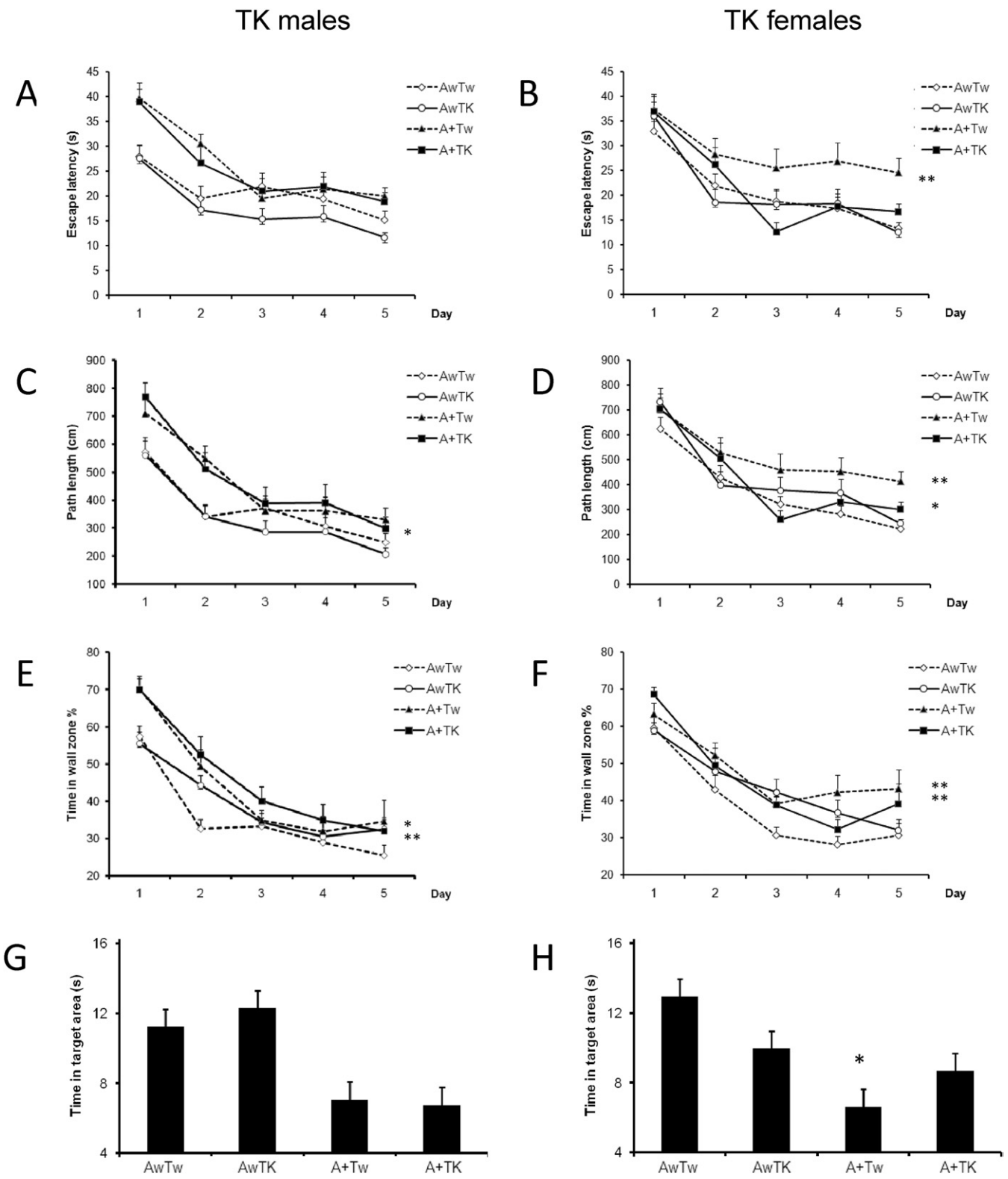

Fig. 6. Morris swim task in APdE9 × TrkB.TK mice at 15 months of age. (A) Escape latency for males; and (B) females. (C) Swim path length for males; and (D) females. (E) Time spent in the zone close to the pool wall (% time) for males; and (F) females. (G) Time spent in the near vicinity of the former platform location during the probe test at the end of Day 5 for males; and (H) females. See Fig. 3 legend for description of statistics.

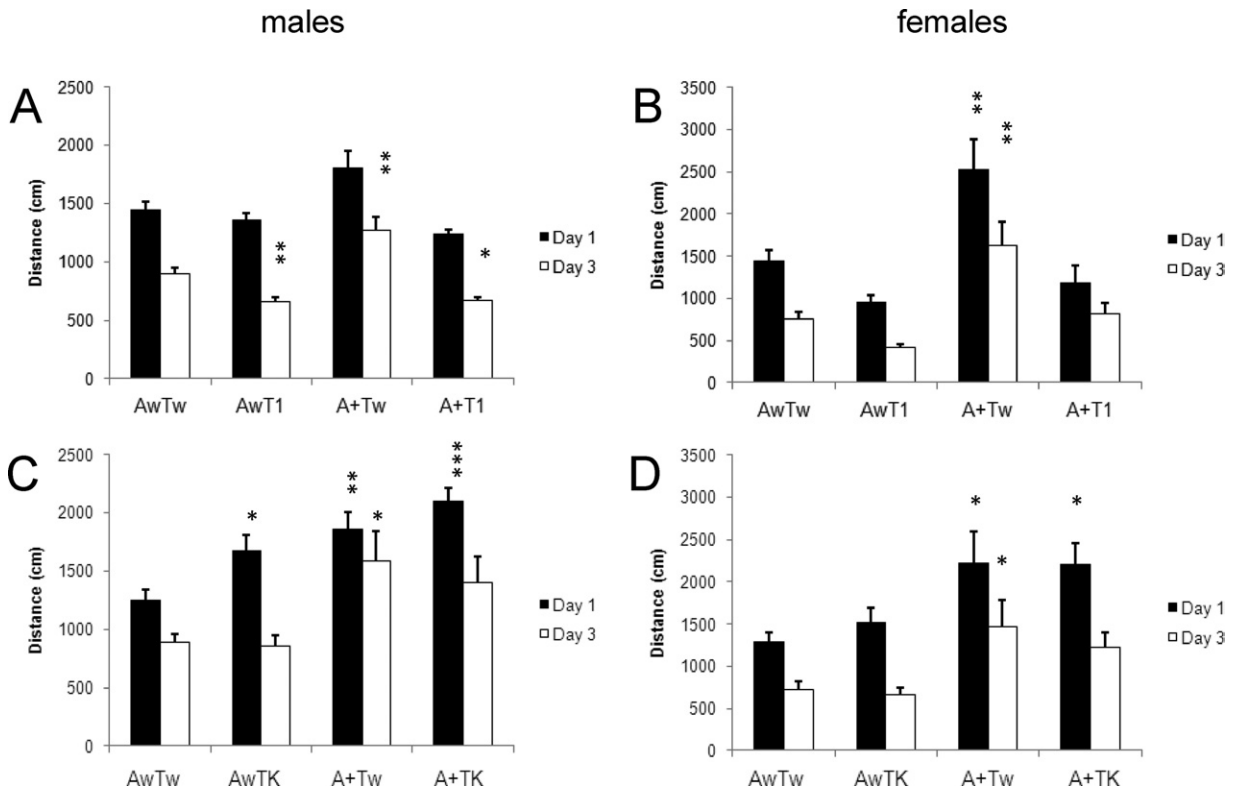

Fig. 7. Ambulatory distance for 2 sessions of free exploration in the test cage on Day 1 and Day 3. (A) APdE9 × TrkB.T1 males, age 12 months; and (B) APdE9 × TrkB.T1 females. (C) APdE9 × TrkB.TK males; and (D) APdE9 × TrkB.TK females. Group means ± standard error of the mean (SEM) are shown. * $p < 0.05$, ** $p < 0.01$, *** $p < 0.001$, Dunnett's post hoc test compared with AwTw group.

($p = 0.04$) than did A+Tw mice, while AwTK and AwTw did not differ ($p > 0.90$, Fig. 6B), suggesting that TrkB.TK overexpression ameliorates the learning deficit in the female APdE9 mice. A similar trend between the groups was also observed in the path length analysis. Paths used by A+ mice were longer (males: $F(1,46) = 15.7$, $p < 0.001$; females: $F(1,45) = 7.1$, $p = 0.01$), while the path followed by the TK mice was not significantly different from the other groups ($p > 0.39$; Fig. 6C and D). However, among female mice the A+TK group outperformed the A+Tw group, while AwTK mice were inferior to AwTw mice (Fig. 6D). This resulted in a significant interaction between the APdE9 and TrkB.TK genotypes ($F(1,45) = 7.9$, $p = 0.007$).

Both 15-month-old male ($F(1,46) = 9.9$, $p = 0.003$) and female ($F(1,45) = 7.1$, $p = 0.01$) A+ mice spent more time in the wall zone than did Aw mice, whereas TrkB.TK overexpression had no effect ($p > 0.35$; Fig. 6E and F). Analysis of search bias in the probe trial also showed both male ($F(1,46) = 7.0$, $p = 0.01$) and female ($F(1,45) = 3.6$, $p = 0.06$) A+ mice searched less time for the platform in its right location than Aw mice Fig. 6G and H, whereas TrkB.TK overexpression had no effect on the search bias ($p > 0.70$).

Taken together, these data indicate that transgenic modulation of TrkB has a relatively small but consistent influence on the acquisition phase of a spatial navigation task, while not influencing the final spatial search bias in the probe task. Our observations lend support to the hypothesis that enhanced TrkB signaling ameliorates spatial learning impairment of APdE9 mice whereas inhibited TrkB signaling aggravates it.

3.6. Overexpression of TrkB isoforms modulates the APdE9-induced increase in exploratory activity

Mice carrying the APdE9 transgene showed significantly increased exploratory activity compared with corresponding wild type littermates, as revealed by the increase in ambulatory distance (gross horizontal locomotion) during the first 10-minute session in a new test cage (Fig. 7A and B). This was observed in both sexes and both ages when A+Tw were compared with AwTw mice (males 12 months: $t_{25} = 2.3$, $p = 0.03$; females 12 months: $t_{21} = 2.6$, $p = 0.02$; males 15 months: $t_{23} = 3.6$, $p = 0.001$; females 15 months: $t_{25} = 2.6$, $p = 0.02$).

In general, TrkB.T1 overexpression decreased locomotion in both A+ and Aw mice (males 12 months: $F(1,51) = 14.0$, $p < 0.001$; females 12 months: $F(1,43) = 16.2$, $p < 0.001$; Fig. 7A and B). However, among male mice the decrease was more pronounced in A+ than Aw mice, resulting in significant interaction between APdE9 and TrkB.T1 genotypes ($F(1,51) = 7.5$, $p = 0.009$). The same

trend was observed in female mice but it did not reach significance ($p > 0.07$). Thus it appears that in the double transgenic A+T1 mice, TrkB.T1 overexpression attenuated the increased locomotor activity produced by the APdE9 genotype (Fig. 7A and B).

All mice moved significantly less during the second session in the test cage 48 hours later, indicating habituation to the environment. Notably, T1 females displayed less habituation than Aw females, resulting in a significant TrkB.T1 by session interaction ($F(1,51) = 7.3$, $p = 0.01$; Fig. 7B), while APdE9 genotype had no effect on habituation ($p > 0.82$). No differences in habituation were found among the male groups.

In general, TrkB.TK overexpression in 15-month-old mice resulted in a moderate increase in exploratory locomotion during the first visit to the test cage in both A+ and Aw groups; this effect was significant in males ($F(1,47) = 7.2$, $p = 0.01$) but not in females ($p > 0.55$). In addition, TK mice habituated more rapidly to the novel environment and reduced their exploratory activity more than Tw mice, resulting in a TrkB.TK × day interaction (males: $F(1,47) = 5.4$, $p = 0.03$; females: $F(1,46) = 3.7$, $p = 0.06$; Fig. 7C and D). There was no interaction between TrkB.TK and APdE9 genotypes.

3.7. Neither TrkB.T1 nor TrkB.TK overexpression affects amyloid accumulation in APdE9 mice

The amyloid plaque load in the septal (dorsal) hippocampus of A+Tw male mice at 12 months of age was 2.9 ± 0.2% (mean ± standard error of the mean [SEM]) of total area of the sections studied, and 3.1 ± 0.3% in A+T1 mice. This difference was not significant ($p = 0.60$). As expected, a higher amyloid load was found in 15-month-old male mice overexpressing the amyloid transgene alone (A+Tw: 5.7 ± 0.4%, mean ± SEM). However, double transgenic mice overexpressing the APdE9 and the full-length TrkB transgenes showed a similar amyloid load (A+TK: 5.9 ± 0.4%; $p = 0.77$), suggesting that overexpression of neither TrkB.T1 nor TrkB.TK had any significant effect on the amyloid accumulation in the brains of APdE9 mice.

4. Discussion

The present study investigated the potential role of BDNF signaling in AD by crossing APPswe/PS1dE9 double transgenic (APdE9) AD model mice with mice overexpressing either full-length TrkB receptor or its dominant-negative TrkB.T1 isoform in the brain. Previous studies have shown that overexpression of TrkB improves spatial memory in mice (Koponen et al., 2004) whereas overexpression of TrkB.T1 slightly impairs it (Saarelainen et al., 2000b). Our results show that TrkB.T1 overexpression further impairs cognitive function of APdE9 mice, whereas overexpression of the functional TrkB isoform ameliorates the cognitive deficit, which is consistent with the idea that the cognitive function of APdE9 mice is sensitive to the level of TrkB signaling in brain. We also discovered an age-dependent increase in the expression of TrkB.T1 in the brains of APdE9 mice, which is in agreement with reports of increased TrkB.T1 levels in postmortem findings in AD brains (Connor et al., 1996; Ferrer et al., 1999). Furthermore, we found that exposure of cultured cortical neurons to Aβ brought about a change in the ratio of full-length to truncated TrkB isoforms to favor the dominant-negative T1 isoform. Collectively, these results are consistent with the notion that interaction of Aβ and BDNF signaling may play a significant role in the pathophysiology and cognitive deficits of AD.

Here we show that APdE9 mice mimic the increase in proportion of nonsignaling truncated TrkB.T1 receptors over full-length Trk.TK receptors as has been reported in AD patients (Connor et al., 1996; Ferrer et al., 1999). This increase is most likely associated with amyloid accumulation as it is absent in 3-month-old mice with no amyloid plaques and is most prominent in cortical areas with the highest amyloid plaque load. This notion is in agreement with postmortem findings in AD brains, where increased levels of TrkB.T1 are found in senile plaques (Connor et al., 1996) as well as reactive glial cells surrounding plaques (Ferrer et al., 1999). Furthermore, the present findings in cultured cortical and hippocampal neurons lend direct support to the primary role of Aβ in bringing about the increase in TrkB.T1 levels. In contrast to reported AD brain pathology, however, the full-length TrkB.TK receptor levels also showed a tendency to increase with increasing amyloid load in APdE9, but to a lesser extent than those of TrkB.T1 levels. Intriguingly, TrkB.TK immunoreactivity in AD brains was largely decreased in tangle-bearing neurons (Ferrer et al., 1999) that are absent in APP transgenic mice, which may fully account for this difference. In any event, the amyloid accumulation in APdE9 mice resulted in the same shift of TK/T1 balance as observed in AD brains.

Although overexpression of TrkB.T1 versus TrkB.TK had in general the expected opposite effects on assessed behavioral parameters, many of the effects are gender-dependent. Whereas TrkB.TK overexpression enhanced spatial learning mainly in APdE9 female mice, the TrkB.T1 effect on exploratory activity was much more pronounced in males. Consistent with these behavioral observations, we found that the effects of TrkB.T1 versus TrkB.TK overexpression on TrkB dependent signaling pathways were not exactly opposite. We focused in our analysis the PI3K-Akt and mitogen-activated protein kinase (MEK)-ERK pathways, dependent on the Shc docking protein that has been pinpointed as the main interaction site for Aβ with the TrkB receptor (Tong et al., 2004). In general we found relatively few changes in signaling phosphoproteins in comparing TrkB.T1 and TrkB.TK effects. This may simply reflect the fact that the brains were collected when the animals were idling in their home cage and not immediately after a chal-

lenging memory task. Furthermore, we have recently observed that the behavioral and biochemical phenotype of both of these mouse strains is reduced in the C57BL6/J background used here when compared with the mixed CDF1 background used in the previous studies (Koponen et al., 2004; Saarelainen et al., 2000a, 2000b) the only significant effect we found related to TrkB.TK overexpression was a change in the levels of phosphorylated CREB (Ser^{133}), which is consistent with our earlier observations (Semenov et al., 2006). TrkB.T1 overexpression did not affect signaling via MEK-ERK, but significantly changed signaling in the PI3K-Akt pathway both in the cortex and hippocampus. This is consistent with a report on the trisomy 16 mouse model of Down syndrome (also overexpressing APP) demonstrating selective activation of PI3K-Akt pathway with BDNF application to primary neurons of these mice with robust upregulation of TrkB.T1 receptor (Dorsey et al., 2006). In contrast to pathway selective effects of TrkB receptor overexpression, APdE9 genotype was associated with phosphoprotein changes in both PI3K-Akt and MEK-ERK pathways.

The phenotype of APdE9 mice revealed in the present study was consistent with earlier findings in APPswe transgenic mice showing age-independent hyperactivity (King and Arendash, 2002; Ognibene et al., 2005) and impaired spatial memory (Hsiao et al., 1996; Minkeviciene et al., 2008; Puoliväli et al., 2002). Both features were extremely robust and could be observed in both genders. To date, however there is little evidence to suggest what the molecular neuropathology underlying this hyperactivity in APPswe transgenic mice is, but its age-independent nature suggests that it is independent of amyloid accumulation. In support of this, a transgenic mouse expressing segmental trisomy for all human chromosome 21-homologous regions of mouse chromosome 16 including APP displays hyperactivity in the absence of amyloid plaque formation (Sago et al., 2000). Also our own unpublished findings in young adult APPswe single mutant mice that develop amyloid plaques only after 20 months of age (Borchelt et al., 1997) confirm hyperactivity in this mouse independent of amyloid plaques. Hyperactivity in APPswe mice has been linked with general behavioral disinhibition and increased serotonin turnover in the frontal cortex (Adriani et al., 2006), and one of the earliest synaptic changes in APdE9 mice is the loss of serotonin terminals in the neocortex (Liu et al., 2008). The interaction of TrkB.T1 with the APdE9-linked hyperactivity could thus happen at the level of cortical monoamine terminals.

In contrast to hyperactivity, age-related spatial memory deficit in APPswe mice is clearly related to the presence of amyloid-β (Aβ) in the hippocampus, but does not necessarily correlate with the amyloid plaque load (Puoliväli et al., 2002; Westerman et al., 2002). There is accumulating evidence to suggest that the amyloid plaque load may rather be a surrogate marker for some toxic forms of soluble Aβ aggregates that account for the spatial memory deficit (Lesné et al., 2006). It is notable that the effects of manipulating TrkB receptors were most obvious during the acquisition of spatial navigation, which involves not only hippocampal-dependent spatial memory but also adaptation of an effective coping strategy (thigmotaxis), which is more closely related to frontal cortical functions. In contrast, TrkB receptor manipulation did not affect search bias which is considered the most selective measure for hippocampal-dependent spatial memory (Wolfer and Lipp, 1992). It is also worth noting that in APdE9 mice the memory enhancing effect of TrkB.TK was more robust than the memory impairing effect of TrkB.T1. This is entirely consistent with the notion that the T1/TK ratio was already significantly increased in the APdE9 mice, particularly in the frontal cortex.

In conclusion, the present study lends support to the contention that impaired BDNF signaling plays a role in synaptic pathophysiology and memory loss in Alzheimer's disease. In particular, postmortem studies have indicated that the number of tyrosine kinase coupled full-length TrkB receptors decrease while the number of truncated TrkB receptor increase in AD brains. The changes are likely caused by accumulation of Aβ peptide, as incubation of cultured cortical neurons with Aβ induced similar changes in TrkB receptor levels. In addition, amyloid pathology in the APdE9 transgenic mouse results in a similar imbalance in the full-length/truncated TrkB receptor levels in an age-dependent manner. A recent study (Nagahara et al., 2009) showed that delivery of BDNF gene via a viral vector into the entorhinal cortex reversed synaptic loss and restored spatial learning deficit in another transgenic mouse model of AD without altering brain amyloid load itself, thus demonstrating the therapeutic potential of increasing brain BDNF levels in AD. The present study complements these findings by demonstrating the importance of TrkB receptor level changes in terms of receptor isoforms. An increase in truncated T1 receptors through a genetic manipulation impaired the already compromised spatial memory of APdE9 mice, whereas increase in full-length TK receptor ameliorates the deficit. Treatments that could normalize the TK/T1 receptor ratio would thus also likely have a beneficial effect in the human disease.

Disclosure statement

The authors disclose no conflicts of interest.

The experiments were conducted according to the Council of Europe (Directive 86/609) and Finnish guidelines, and approved by the State Provincial Office of Eastern Finland.

Acknowledgements

We thank L. Alhonen (A. I. Virtanen Insitute, Univ. Eastern, Finland), D. Borchelt (Univ. Florida, FL, USA), and J. Jankowsky (Baylor College of Medicine, Houston,

TX, USA) for the breeder mice for this study, and H.G. Franquelim and M.A.R.B. Castanho for assistance with AFM. This work was supported by EU 6th Framework program grant FP6-037831, EU 7th Framework program grant HEALTH-F2-2007-201159, Fundação para a Ciência e Tecnologia (Portugal), EMBO Installation Grant, Marie Curie International Reintegration Grant (Neurofold), FCT fellowship SFRH/BPD/64,702/2009, Sigrid Juselius Foundation (Finland), and the Academy of Finland.

Appendix A. Supplementary data

Supplementary data associated with this article can be found, in the online version, at doi:10.1016/j.neurobiolaging.2011.11.006.

References

Adriani, W., Ognibene, E., Heuland, E., Ghirardi, O., Caprioli, A., Laviola, G., 2006. Motor impulsivity in APP-SWE mice: a model of Alzheimer's disease. Behav. Pharmacol. 17, 525–533.

Aizenstein, H.J., Nebes, R.D., Saxton, J.A., Price, J.C., Mathis, C.A., Tsopelas, N.D., Ziolko, S.K., James, J.A., Snitz, B.E., Houck, P.R., Bi, W., Cohen, A.D., Lopresti, B.J., DeKosky, S.T., Halligan, E.M., Klunk, W.E., 2008. Frequent amyloid deposition without significant cognitive impairment among the elderly. Arch. Neurol. 2008, 1509–1517.

Arancio, O., Chao, M.V., 2007. Neurotrophins, synaptic plasticity and dementia. Curr. Opin. Neurobiol. 17, 325–330.

Bonfoco, E., Krainc, D., Ankarcrona, M., Nicotera, P., Lipton, S.A., 1995. Apoptosis and necrosis: two distinct events induced, respectively, by mild and intense insults with *N*-methyl-d-aspartate or nitric oxide/superoxide in cortical cell cultures. Proc. Natl. Acad. Sci. USA 92, 7162–7166.

Borchelt, D.R., Ratovitski, T., van Lare, J., Lee, M.K., Gonzales, V., Jenkins, N.A., Copeland, N.G., Price, D.L., Sisodia, S.S., 1997. Accelerated amyloid deposition in the brains of transgenic mice coexpressing mutant presenilin 1 and amyloid precursor proteins. Neuron 19, 939–945.

Brewer, G.J., Torricelli, J.R., Evege, E.K., Price, P.J., 1993. Optimized survival of hippocampal neurons in B27-supplemented Neurobasal, a new serum-free medium combination. J. Neurosci. Res. 35, 567–576.

Burbach, G.J., Hellweg, R., Haas, C.A., Del Turco, D., Deicke, U., Abramowski, D., Jucker, M., Staufenbiel, M., Deller, T., 2004. Induction of brain-derived neurotrophic factor in plaque-associated glial cells of aged APP 23 transgenic mice. J. Neurosci. 24, 2421–2430.

Castrén, E., Tanila, H., 2006. Neurotrophins and dementia—keeping in touch. Neuron 51, 1–3.

Connor, B., Dragunow, M., 1998. The role of neuronal growth factors in neurodegenerative disorders of the human brain. Brain Res. Brain Res. Rev. 27, 1–39.

Connor, B., Young, D., Lawlor, P., Gai, W., Waldvogel, H., Faull, R.L., Dragunow, M., 1996. Trk receptor alterations in Alzheimer's disease. Brain Res. Mol. Brain Res. 42, 1–17.

Connor, B., Young, D., Yan, Q., Faull, R.L., Synek, B., Dragunow, M., 1997. Brain-derived neurotrophic factor is reduced in Alzheimer's disease. Brain Res. Mol. Brain Res. 49, 71–81.

Dorsey, S.G., Renn, C.L., Carim-Todd, L., Barrick, C.A., Bambrick, L., Krueger, B.K., Ward, C.W., Tessarollo, L., 2006. In vivo restoration of physiological levels of truncated TrkB.T1 receptor rescues neuronal cell death in a trisomic mouse model. Neuron 51, 21–28.

Eide, F.F., Vining, E.R., Eide, B.L., Zang, K., Wang, X.Y., Reichardt, L.F., 1996. Naturally occurring truncated TrkB receptors have dominant inhibitory effects on brain-derived neurotrophic factor signaling. J. Neurosci. 16, 3123–3129.

Ferrer, I., Marín, C., Rey, M.J., Ribalta, T., Goutan, E., Blanco, R., Tolosa, E., Martí, E., 1999. BDNF and full-length and truncated TrkB expression in Alzheimer disease. Implications in therapeutic strategies. J. Neuropathol. Exp. Neurol. 58, 729–739.

Garcia-Alloza, M., Robbins, E.M., Zhang-Nunes, S.X., Purcell, S.M., Betensky, R.A., Raju, S., Prada, C., Greenberg, S.M., Bacskai, B.J., Frosch, M.P., 2006. Characterization of amyloid deposition in the APPswe/PS1dE9 mouse model of Alzheimer disease. Neurobiol. Dis. 24, 516–524.

Haapasalo, A., Koponen, E., Hoppe, E., Wong, G., Castrén, E., 2001. Truncated TrkB.T1 is dominant negative inhibitor of TrkB.TK+-mediated cell survival. Biochem. Biophys. Res. Commun. 280, 1352–1358.

Hsiao, K., Chapman, P., Nilsen, S., Eckman, C., Harigaya, Y., Younkin, S., Yang, F., Cole, G., 1996. Correlative memory deficits, Abeta elevation, and amyloid plaques in transgenic mice. Science 274, 99–102.

Huang, E.J., Reichardt, L.F., 2001. Neurotrophins: roles in neuronal development and function. Annu. Rev. Neurosci. 24, 677–736.

Jankowsky, J.L., Fadale, D.J., Anderson, J., Xu, G.M., Gonzales, V., Jenkins, N.A., Copeland, N.G., Lee, M.K., Younkin, L.H., Wagner, S.L., Younkin, S.G., Borchelt, D.R., 2004. Mutant presenilins specifically elevate the levels of the 42 residue beta-amyloid peptide in vivo: evidence for augmentation of a 42-specific gamma secretase. Hum. Mol. Genet. 13, 159–170.

Kadir, A., Almkvist, O., Forsberg, A., Wall, A., Engler, H., Långström, B., Nordberg, A., 2012. Dynamic changes in PET amyloid and FDG imaging at different stages of Alzheimer's disease. Neurobiol. Aging 33, 198.e1–198.e14.

Karpova, N.N., Lindholm, J., Pruunsild, P., Timmusk, T., Castrén, E., 2009. Long-lasting behavioural and molecular alterations induced by early postnatal fluoxetine exposure are restored by chronic fluoxetine treatment in adult mice. Eur. Neuropsychopharmacol. 19, 97–108.

King, D.L., Arendash, G.W., 2002. Behavioral characterization of the Tg2576 transgenic model of Alzheimer's disease through 19 months. Physiol. Behav. 75, 627–642.

Koponen, E., Võikar, V., Riekki, R., Saarelainen, T., Rauramaa, T., Rauvala, H., Taira, T., Castrén, E., 2004. Transgenic mice overexpressing the full-length neurotrophin receptor TrkB exhibit increased activation of the TrkB-PLCgamma pathway, reduced anxiety, and facilitated learning. Mol. Cell. Neurosci. 26, 166–181.

Lesné, S., Koh, M.T., Kotilinek, L., Kayed, R., Glabe, C.G., Yang, A., Gallagher, M., Ashe, K.H., 2006. A specific amyloid-beta protein assembly in the brain impairs memory. Nature 440, 352–357.

Liu, Y., Yoo, M.J., Savonenko, A., Stirling, W., Price, D.L., Borchelt, D.R., Mamounas, L., Lyons, W.E., Blue, M.E., Lee, M.K., 2008. Amyloid pathology is associated with progressive monoaminergic neurodegeneration in a transgenic mouse model of Alzheimer's disease. J. Neurosci. 28, 13805–13814.

Minichiello, L., 2009. TrkB signalling pathways in LTP and learning. Nat. Rev. Neurosci. 10, 850–860.

Minichiello, L., Korte, M., Wolfer, D., Kühn, R., Unsicker, K., Cestari, V., Rossi-Arnaud, C., Lipp, H.P., Bonhoeffer, T., Klein, R., 1999. Essential role for TrkB receptors in hippocampus-mediated learning. Neuron 24, 401–414.

Minkeviciene, R., Ihalainen, J., Malm, T., Matilainen, O., Keksa-Goldsteine, V., Goldsteins, G., Iivonen, H., Leguit, N., Glennon, J., Koistinaho, J., Banerjee, P., Tanila, H., 2008. Age-related decrease in stimulated glutamate release and vesicular glutamate transporters in APP/PS1 transgenic and wild-type mice. J. Neurochem. 105, 584–594.

Nagahara, A.H., Merrill, D.A., Coppola, G., Tsukada, S., Schroeder, B.E., Shaked, G.M., Wang, L., Blesch, A., Kim, A., Conner, J.M., Rockenstein, E., Chao, M.V., Koo, E.H., Geschwind, D., Masliah, E., Chiba, A.A., Tuszynski, M.H., 2009. Neuroprotective effects of brain-derived

neurotrophic factor in rodent and primate models of Alzheimer's disease. Nat. Med. 15, 331–337.

Nilsson, M.R., 2004. Techniques to study amyloid fibril formation in vitro. Methods 34, 151–160.

Ognibene, E., Middei, S., Daniele, S., Adriani, W., Ghirardi, O., Caprioli, A., Laviola, G., 2005. Aspects of spatial memory and behavioral disinhibition in Tg2576 transgenic mice as a model of Alzheimer's disease. Behav. Brain Res. 156, 225–232.

Peng, S., Garzon, D.J., Marchese, M., Klein, W., Ginsberg, S.D., Francis, B.M., Mount, H.T., Mufson, E.J., Salehi, A., Fahnestock, M., 2009. Decreased brain-derived neurotrophic factor depends on amyloid aggregation state in transgenic mouse models of Alzheimer's disease. J. Neurosci. 29, 9321–9329.

Peng, S., Wuu, J., Mufson, E.J., Fahnestock, M., 2005. Precursor form of brain-derived neurotrophic factor and mature brain-derived neurotrophic factor are decreased in the pre-clinical stages of Alzheimer's disease. J. Neurochem. 93, 1412–1421.

Phillips, H.S., Hains, J.M., Armanini, M., Laramee, G.R., Johnson, S.A., Winslow, J.W., 1991. BDNF mRNA is decreased in the hippocampus of individuals with Alzheimer's disease. Neuron 7, 695–702.

Puoliväli, J., Wang, J., Heikkinen, T., Heikkilä, M., Tapiola, T., van Groen, T., Tanila, H., 2002. Hippocampal A beta 42 levels correlate with spatial memory deficit in APP and PS1 double transgenic mice. Neurobiol. Dis. 9, 339–347.

Rantamäki, T., Hendolin, P., Kankaanpää, A., Mijatovic, J., Piepponen, P., Domenici, E., Chao, M.V., Männistö, P.T., Castrén, E., 2007. Pharmacologically diverse antidepressants rapidly activate brain-derived neurotrophic factor receptor TrkB and induce phospholipase-Cgamma signaling pathways in mouse brain. Neuropsychopharmacology 32, 2152–2162.

Rodrigues, C.M., Solá, S., Silva, R., Brites, D., 2000. Bilirubin and amyloid-β peptide induce cytochrome *c* release through mitochondrial membrane permeabilization. Mol. Med. 6, 936–946.

Rose, C.R., Blum, R., Pichler, B., Lepier, A., Kafitz, K.W., Konnerth, A., 2003. Truncated TrkB-T1 mediates neurotrophin-evoked calcium signalling in glia cells. Nature 426, 74–78.

Saarelainen, T., Hendolin, P., Lucas, G., Koponen, E., Sairanen, M., MacDonald, E., Agerman, K., Haapasalo, A., Nawa, H., Aloyz, R., Ernfors, P., Castrén, E., 2003. Activation of the TrkB neurotrophin receptor is induced by antidepressant drugs and is required for antidepressant-induced behavioral effects. J. Neurosci. 23, 349–357.

Saarelainen, T., Lukkarinen, J.A., Koponen, S., Gröhn, O.H., Jolkkonen, J., Koponen, E., Haapasalo, A., Alhonen, L., Wong, G., Koistinaho, J., Kauppinen, R.A., Castrén, E., 2000a. Transgenic mice overexpressing truncated TrkB neurotrophin receptors in neurons show increased susceptibility to cortical injury after focal cerebral ischemia. Mol. Cell. Neurosci. 16, 87–96.

Saarelainen, T., Pussinen, R., Koponen, E., Alhonen, L., Wong, G., Sirviö, J., Castrén, E., 2000b. Transgenic mice overexpressing truncated TrkB neurotrophin receptors in neurons have impaired long-term spatial memory but normal hippocampal LTP. Synapse 38, 102–104.

Sago, H., Carlson, E.J., Smith, D.J., Rubin, E.M., Crnic, L.S., Huang, T.T., Epstein, C.J., 2000. Genetic dissection of region associated with behavioral abnormalities in mouse models for Down syndrome. Pediatr. Res. 48, 606–613.

Savonenko, A., Xu, G.M., Melnikova, T., Morton, J.L., Gonzales, V., Wong, M.P., Price, D.L., Tang, F., Markowska, A.L., Borchelt, D.R., 2005. Episodic-like memory deficits in the APPswe/PS1dE9 mouse model of Alzheimer's disease: relationships to beta-amyloid deposition and neurotransmitter abnormalities. Neurobiol. Dis. 18, 602–617.

Schindowski, K., Belarbi, K., Buée, L., 2008. Neurotrophic factors in Alzheimer's disease: role of axonal transport. Genes Brain Behav. 7 suppl 1, 43–56.

Schulte-Herbrüggen, O., Eckart, S., Deicke, U., Kühl, A., Otten, U., Danker-Hopfe, H., Abramowski, D., Staufenbiel, M., Hellweg, R., 2008. Age-dependent time course of cerebral brain-derived neurotrophic factor, nerve growth factor, and neurotrophin-3 in APP23 transgenic mice. J. Neurosci. Res. 12, 2774–2783.

Selkoe, D.J., 2002. Alzheimer's disease is a synaptic failure. Science 298, 789–791.

Semenov, A., Goldsteins, G., Castrén, E., 2006. Phosphoproteomic analysis of neurotrophin receptor TrkB signaling pathways in mouse brain. Cell. Mol. Neurobiol. 26, 163–175.

Slee, E.A., Zhu, H., Chow, S.C., MacFarlane, M., Nicholson, D.W., Cohen, G.M., 1996. Benzyloxycarbonyl-Val-Ala-Asp (OMe) fluoromethylketone (Z-VAD.FMK) inhibits apoptosis by blocking the processing of CPP32. Biochem. J. 315, 21–4.

Szapacs, M.E., Numis, A.L., Andrews, A.M., 2004. Late onset loss of hippocampal 5-HT and NE is accompanied by increases in BDNF protein expression in mice co-expressing mutant APP and PS1. Neurobiol. Dis. 16, 572–580.

Tong, L., Balazs, R., Thornton, P.L., Cotman, C.W., 2004. Beta-amyloid peptide at sublethal concentrations downregulates brain-derived neurotrophic factor functions in cultured cortical neurons. J. Neurosci. 24, 6799–6809.

Van Dam, D., D'Hooge, R., Staufenbiel, M., Van Ginneken, C., Van Meir, F., De Deyn, P.P., 2003. Age-dependent cognitive decline in the APP23 model precedes amyloid deposition. Eur. J. Neurosci. 17, 388–396.

Westerman, M.A., Cooper-Blacketer, D., Mariash, A., Kotilinek, L., Kawarabayashi, T., Younkin, L.H., Carlson, G.A., Younkin, S.G., Ashe, K.H., 2002. The relationship between Abeta and memory in the Tg2576 mouse model of Alzheimer's disease. J. Neurosci. 22, 1858–1867.

Wolfer, D.P., Lipp, H.P., 1992. A new computer program for detailed off-line analysis of swimming navigation in the Morris water maze. J. Neurosci. Methods 41, 65–74.

Zuccato, C., Cattaneo, E., 2009. Brain-derived neurotrophic factor in neurodegenerative diseases. Nat. Rev. Neurol. 5, 311–322.